Equilibrium and Kinetics of NO and CO Chemisorptions on Nonstoichiometric Nickel–Copper Manganites

Christophe Drouet,* Pierre Alphonse,*,[1] José Luis García Fierro,† and Abel Rousset*

*Laboratoire de Chimie des Matériaux Inorganiques et Energétiques, Université Paul Sabatier, 118 Route de Narbonne, 31062 Toulouse Cedex 04, France; and †Instituto de Catálisis y Petroleoquímica, Cantoblanco, 28049 Madrid, Spain

The equilibrium and kinetics of adsorption of NO and CO on nonstoichiometric nickel–copper manganites have been investigated through volumetric measurements. The adsorption isotherms were satisfactorily fitted to the Freundlich equation. The equilibrium coverages at 298 K were found to depend closely on the chemical composition of the oxide; thus, a decrease in the coverage beyond a maximum copper extent was observed. The adsorption isotherms of NO at various temperatures in the range from 298 to 473 K showed that the equilibrium coverage decreases with increasing temperature. This behavior enabled us to follow the logarithmic decrease of the heat of adsorption of NO on such surfaces. The adsorptions of NO and CO on surfaces preadsorbed with CO and NO, respectively, were also studied. These experiments showed the ability of NO to displace CO preadsorbed molecules whereas the contrary did not hold, suggesting the existence of common adsorption sites as well as some specific CO adsorption sites. Finally, some kinetic data are reported showing that the experimental adsorption results fit the Elovich equation (with $t_0 \approx 0$), although two distinct rate processes could be identified.

Key Words: **NO; CO; chemisorption; nickel–copper manganites.**

INTRODUCTION

Environmental concerns over air pollution have led to a particular interest in CO oxidation catalysts. An example is the car exhaust engine which produces CO emissions contributing directly to air pollution and smog. The catalytic converters employed today contain a catalytic material which oxidizes CO to CO_2 and also reduces the amount of NO_X and hydrocarbons. The catalytic components included in the cartridges of these converters are platinum, rhodium, and palladium, expensive metals which are deactivated by thermal reactions, cycling operations, and poisons. Thus, the development of new materials with high performance for the above-mentioned reactions are required.

Nonstoichiometric nickel and nickel–copper manganites have already been investigated in previous works (1–3). It was reported (3) that the substitution of part of the manganese cations by copper reinforces the thermal stability of such metastable phases. Recent catalytic experiments have shown that such manganites exhibit high activity toward the CO/O_2 and CO/NO reactions, which is closely related to the nickel and copper contents of the oxides (results to be published).

The aim of the present paper is to investigate the equilibrium and kinetics of the adsorption of NO and CO molecules on nickel–copper manganites. For such a purpose, the adsorption isotherms of NO and CO have been recorded for various chemical compositions to determine the effect of nickel and copper contents on the adsorption properties. The study of NO adsorption at various temperatures was also examined to establish the dependence of the heat of adsorption on surface coverage.

MATERIALS AND METHODS

Preparation of Samples

The oxide systems studied in this work are nonstoichiometric nickel–copper manganites corresponding to the general formula $Ni_xCu_yMn_{3-x-y}O_{4+\delta}$. These are cation-deficient oxides (δ ranging from 0.2 to 0.7) and crystallize in the cubic spinel structure (3). These compounds were synthesized in two steps: (i) coprecipitation of a mixed Ni–Cu–Mn oxalate precursor of desired composition and (ii) thermal decomposition of this precursor at 623 K in air for 6 h (the detailed synthesis is described elsewhere (3)). Such a preparation route permits one to prepare oxides with high specific area ($S_w > 100\ m^2/g$) as shown in Table 1. Manganese oxide was prepared according to the same procedure as above from thermal decomposition of manganese oxalate (α allotropic form), and the phase obtained was $Mn_5O_{8+\delta}$ (3, 4), which does not exhibit the spinel structure (5).

Chemisorption Measurements

A conventional volumetric Pyrex-glass high-vacuum system with greaseless stopcocks capable of maintaining a dynamic vacuum of 10^{-6} Torr (1 Torr = 133.3 Pa) was used. Temperatures were measured with a chromel–alumel thermocouple. Pressure measurements were made by means of an MKS capacitance transducer comprised of a sensor head 310 BHS1000, an electronic unit, and a meter unit. The apparatus had a measuring range of 10^{-3} to 10^3 Torr and an accuracy of 10^{-2} Torr.

TABLE 1
Specific Surface Area, S_w, of the Samples

Oxide composition	S_w (m^2/g)
$Mn_5O_{8+\delta}$	125
$Ni_{0.25}Mn_{2.75}O_{4+\delta}$	165
$Ni_{0.22}Cu_{0.57}Mn_{2.21}O_{4+\delta}$	150
$Ni_{0.25}Cu_{0.38}Mn_{2.37}O_{4+\delta}$	155
$Ni_{0.25}Cu_{0.80}Mn_{1.95}O_{4+\delta}$	150

The total volume of the measuring cell and reactor was about 10 cm^3.

Prior to each adsorption experiment, the sample (50 mg) was outgassed under high vacuum for 1 h at 573 K, and the temperature was then set to the desired value. Such a pretreatment was compulsory to clean the surface; however, it could have led to a slight reduction of the surface. Each adsorption experiment was carried out, after pretreatment, introducing in several successive steps a given pressure of adsorbate in the calibrated volume containing the sample and noting the equilibrium pressure reached after a stabilization time of 3 h. The application of Boyle's law then led easily to the determination of the quantity of gas adsorbed from the value of the equilibrium pressure and that of the calibrated volume.

The adsorption experiments of NO and CO on surfaces preadsorbed with CO and NO respectively were carried out from clean surfaces as follows: (i) exposure of the sample to the first adsorbate at the desired pressure (calculated from adsorption isotherms to correspond to surface saturation), (ii) evacuation of the remaining gas phase under a primary vacuum (ca. 10^{-2} Torr) for 15 min, and (iii) introduction of the second adsorbate at successively increasing pressures.

The kinetics of NO and CO adsorption on the surface of the oxides was investigated following the variation of the pressure measured by the MKS pressure transducer as a function of time after introduction of a given pressure of adsorbate on a clean surface.

RESULTS AND DISCUSSION

Equilibrium of Adsorption

The adsorption isotherms of NO and CO on the nonstoichiometric nickel–copper manganite $Ni_{0.25}Cu_{0.80}Mn_{1.95}O_{4+\delta}$ at 298 and 373 K are reported in Fig. 1 as $N_a = f(P_{eq})$, where N_a is the number of molecules adsorbed per gram of oxide and P_{eq} is the equilibrium pressure of the adsorbate reached. At first glance, the shape of the three isotherms, (a), (b), and (c) corresponding respectively to the adsorptions of NO and CO at 298 and of NO at 373 K, are of type I in the BDDT classification, reaching an equilibrium asymptote from low pressures ($P \approx 50$ Torr). In contrast, the adsorption isotherm of CO at 373 K (curve (d)) deviates clearly from type I. Such a behavior can be explained easily by recalling the exceptional reactivity of these oxides toward CO oxidation, even at room temperature. Therefore, to discriminate between the pure chemisorption and the oxidation process, CO-adsorption experiments on these oxides must be recorded at temperatures not higher than room temperature. However, the isotherm corresponding to CO adsorption at 298 K (curve (b)) still belongs to type I of BDDT classification, despite the activity of the oxide for CO oxidation. It is presumed that the vacuum pretreatment might have reduced the oxide surface to a sufficient extent as to stop its activity toward CO oxidation.

If the data of isotherm (a) in Fig. 1 are replotted in terms of $\ln(N_a) = f(\ln(P_{eq}))$, a correlation coefficient of 0.9988 is obtained, showing the linearity of this plot which is indicative of a Freundlich-type isotherm:

$$N_a = k \cdot P_{eq}^{1/n}, \qquad [1]$$

where n and k are temperature-dependent constants, the values of which can be directly deduced from the slope and intercept of the $\ln(N_a)$ vs $\ln(P_{eq})$ plot.

If the same mathematical treatment is repeated for isotherms (b) and (c), a similar linearity between $\ln(N_a)$ and $\ln(P_{eq})$ is obtained, showing again that the Freundlich equation precisely describes the experimental results. Such a correspondence with the Freundlich equation points out the heterogeneity of the surface, and various other studies on chemisorptions of NO and CO on transition metal oxides (6–8) have also shown the agreement with this isotherm. As expected, isotherm (d) does *not* fit the Freundlich equation since the catalytic oxidation of CO is overimposed to the adsorption process.

As the catalytic properties of the nickel–copper manganites depend closely on the chemical composition of the oxide, the study of the effect of the nickel and copper contents on the quantities of NO and CO chemisorbed appear to be of great relevance. The adsorption isotherms of both adsorbates at 298 K on manganese oxide $Mn_5O_{8+\delta}$, nickel manganite $Ni_{0.25}Mn_{2.75}O_{4+\delta}$, and nickel–copper manganites $Ni_{0.25}Cu_{0.38}Mn_{2.37}O_{4+\delta}$ and $Ni_{0.25}Cu_{0.80}Mn_{1.95}O_{4+\delta}$ are reported in Fig. 2. Nevertheless, it is

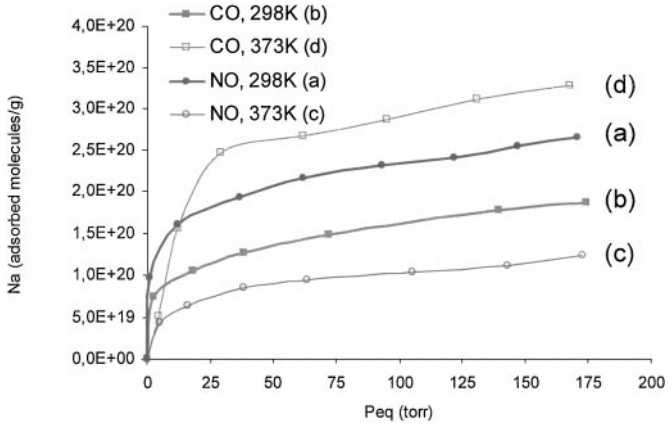

FIG. 1. Adsorption isotherms on $Ni_{0.25}Cu_{0.80}Mn_{1.95}O_{4+\delta}$ of NO at 298 K (a) and 373 K (c) and CO at 298 K (b) and 373 K (d).

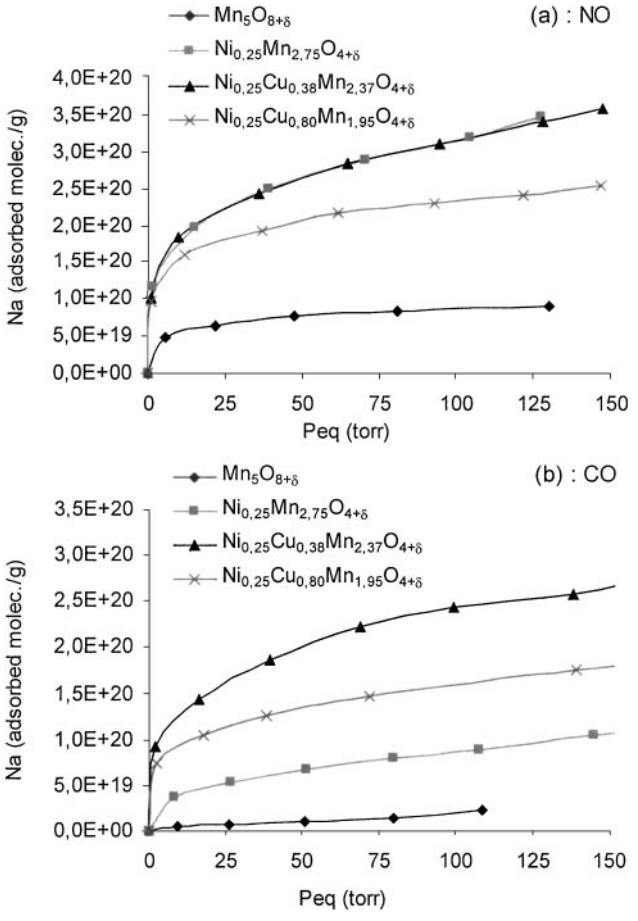

FIG. 2. Adsorption isotherms at 298 K of NO (a) and CO (b) on $Mn_5O_{8+\delta}$, $Ni_{0.25}Mn_{2.75}O_{4+\delta}$, $Ni_{0.25}Cu_{0.38}Mn_{2.37}O_{4+\delta}$, and $Ni_{0.25}Cu_{0.80}Mn_{1.95}O_{4+\delta}$.

emphasized here that the vacuum pretreatment of $Mn_5O_{8+\delta}$ led to a slight change in color of the manganese oxide from black to dark brown, certainly indicative of the reduction, at least partial, of $Mn_5O_{8+\delta}$ to Mn_3O_4. However, the results corresponding to the isotherm obtained for manganese oxide, whichever it was, could bring interesting data to compare to nickel and nickel–copper-containing oxides. Moreover, Mn_3O_4 possesses the spinel structure which is a common point with the other oxides and can thus be taken as good reference oxide.

In the case of NO adsorption, the equilibrium coverage reached on manganese oxide is much smaller than that on nickel-containing manganites, which underlines the influence of nickel on NO chemisorption (Fig. 2a). Furthermore, the comparison of the three nickel-containing oxides with different copper contents shows a slight decrease of the quantity of NO adsorbed with increasing copper content. The little difference among the specific areas of the three oxides (see Table 1) cannot explain, at least completely, this behavior. Figure 2b shows the same conclusion as above, concerning the important influence of nickel, for CO chemisorption. In contrast, the effect of copper on the quantity of CO chemisorbed is different from the case of NO chemisorption. Indeed, the incorporation of copper into the nickel manganite structure leads to an equilibrium coverage of CO more than 3 times larger than that in the absence of Cu. However, a further increase of copper content leads to a decrease of the quantity of CO adsorbed, as can be seen for the $Ni_{0.25}Cu_{0.80}Mn_{1.95}O_{4+\delta}$ sample. A comparison of the results of Figs. 2a and 2b reveals that, for the same oxide, the NO equilibrium coverage is always higher than that obtained for CO (for the same temperature, here, 298 K). The corresponding values of the equilibrium coverages (given by the value of the intercept of the asymptote reached) are reported in Table 2. These results are similar to those of Yao and Shelef (6) obtained for cobalt-containing spinel systems.

TABLE 2
Equilibrium Coverages for NO and CO Adsorption at 298 K

Oxide	Equilibrium coverage (molecules/g) NO	CO
$Mn_5O_{8+\delta}$	0.6×10^{20}	0.2×10^{20}
$Ni_{0.25}Mn_{2.75}O_{4+\delta}$	2.1×10^{20}	0.5×10^{20}
$Ni_{0.25}Cu_{0.38}Mn_{2.37}O_{4+\delta}$	2.2×10^{20}	1.8×10^{20}
$Ni_{0.25}Cu_{0.80}Mn_{1.95}O_{4+\delta}$	1.9×10^{20}	1.2×10^{20}

As stated above, the high reactivity toward CO oxidation of the oxides studied in this work impeded us from monitoring the evolution of the equilibrium coverage of CO at temperatures above room temperature, and the equipment used in this study did not allow us to work at lower temperatures. In contrast, NO chemisorption could be investigated at temperatures higher than room temperature, and the results reported hereafter concern experiments conducted in the temperature range from 298 to 473 K.

Figure 3a reports the adsorption isotherms of NO on $Ni_{0.25}Cu_{0.80}Mn_{1.95}O_{4+\delta}$ at 298, 333, 373, and 473 K. As can be seen, the NO equilibrium coverage decreases progressively when the temperature increases. The shape analysis of these isotherms shows that Eq. [1] is still valid, and the corresponding parameters of Freundlich's isotherm (n and k) are given in Table 3. As a general trend, both n and k decrease with increasing temperature; in particular, n tends to unity, approaching Henry's law. The data of Fig. 3a were replotted in Fig. 3b in terms of $\ln(N_a)$ vs $\ln(P_{eq})$, and the intersection point of all the isotherms, deduced by extrapolation, gives the value of the monolayer coverage $N_m \cong 1.05 \times 10^{21}$ molecules of NO/g. It can be noted

TABLE 3
Freundlich Parameters (n, k) and Heat of Adsorption for Monolayer Coverage ΔH_m in the Case of NO Adsorptions on $Ni_{0.25}Cu_{0.80}Mn_{1.95}O_{4+\delta}$ at 298, 333, 373, and 473 K

T (K)	298	333	373	473
n	5.4	3.2	2.5	1.9
k (molecules/g)	10.1×10^{19}	4.70×10^{19}	2.81×10^{19}	0.85×10^{19}
$\Delta H_m = nRT/(1 - rT)$ (kj/mol)	23.0	16.6	16.2	22.1
r	$r \sim 1.4 \times 10^{-3}$			

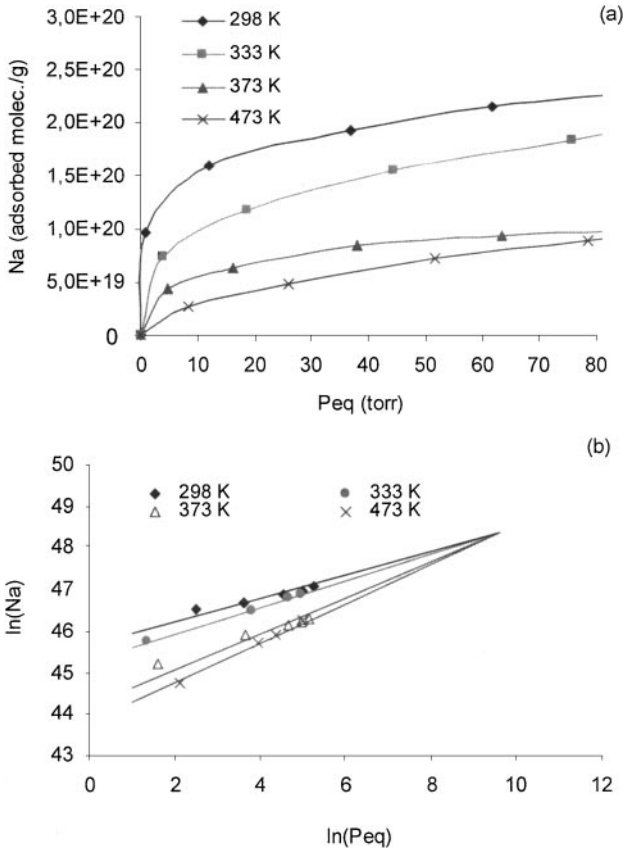

FIG. 3. Adsorption isotherms of NO on $Ni_{0.25}Cu_{0.80}Mn_{1.95}O_{4+\delta}$ at 298, 333, 373, and 473 K as (a) $N_a = f(P_{eq})$ and (b) $\ln(N_a) = f(\ln(P_{eq}))$.

that this value leads to a surface area covered by NO of $\approx$130 m^2/g (taking a value of 0.125 nm^2 for the cross section of the NO molecule (9)) which is close to the specific surface area (150 m^2/g) derived from the nitrogen adsorption isotherms at 77 K.

The variation of the adsorption heat of NO with coverage can be directly determined from Freundlich's theory by the relation

$$\Delta H = -\Delta H_m \cdot \ln\theta, \qquad [2]$$

where $\theta = N_a/N_m$ and ΔH_m can be calculated from n with the relation

$$\Delta H_m = nRT/(1 - rT), \qquad [3]$$

where r is a correcting parameter introduced by Halsey (10), taking into account the small variation of ΔH_m with T. The values of ΔH_m and r are also reported in Table 3.

On the other hand, the heat of adsorption, at constant coverage θ, can be derived from the Clausius–Clapeyron equation

$$\left(\frac{d\ln P}{d\,1/T}\right)_\theta = -\frac{\Delta H}{R}. \qquad [4]$$

Figure 4 shows the variation of ΔH with the NO coverage obtained by both methods (using Eqs. [2] and [4]), taking a

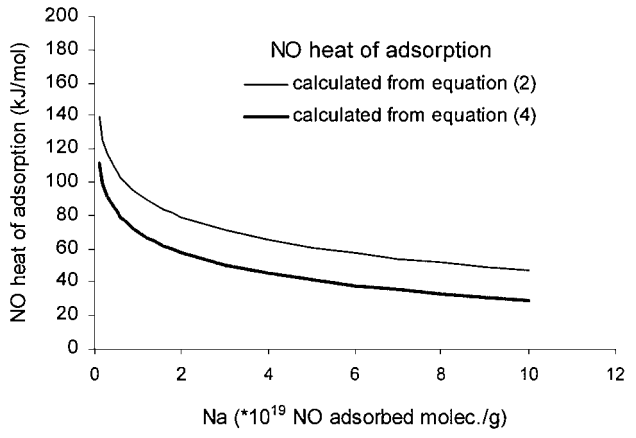

FIG. 4. NO heat of adsorption on $Ni_{0.25}Cu_{0.80}Mn_{1.95}O_{4+\delta}$ calculated from Eqs. [2] and [4] (see text).

mean value of $\Delta H_m = 20$ kJ/mol. As expected in the case of Freundlich-type isotherms, the experimental heat of adsorption decreases logarithmically with the coverage and the two curves are in quite good agreement within the experimental errors.

From the adsorption isotherms, a set of isobars was determined and some of them are plotted in Fig. 5, showing that the experimental data in the temperature range 298–473 K correspond to the descending branch of the isobars, i.e., the chemisorptive part. These descending branches begin near room temperature, which recalls the results obtained by Peña *et al.* (11) for the chemisorption of NO on the manganese-containing perovskite $LaMnO_3$.

To investigate the eventual competitive behavior of NO and CO molecules for the surface adsorption sites, the adsorption of each gas was studied in the same conditions as before, but on surfaces saturated with the other adsorbate. The results presented below are relative to competitive adsorption at 298 K on the mixed oxide $Ni_{0.25}Cu_{0.80}Mn_{1.95}O_{4+\delta}$. Figures 6a and 6b give the evolution of the equilibrium pressure P_{eq} of NO and

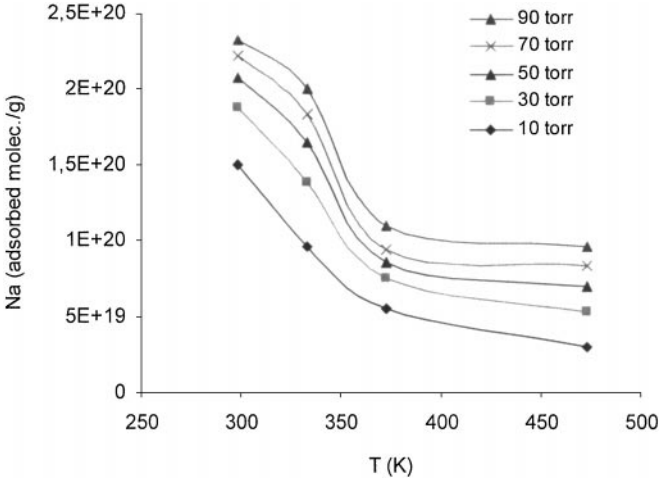

FIG. 5. NO adsorption isobars on $Ni_{0.25}Cu_{0.80}Mn_{1.95}O_{4+\delta}$.

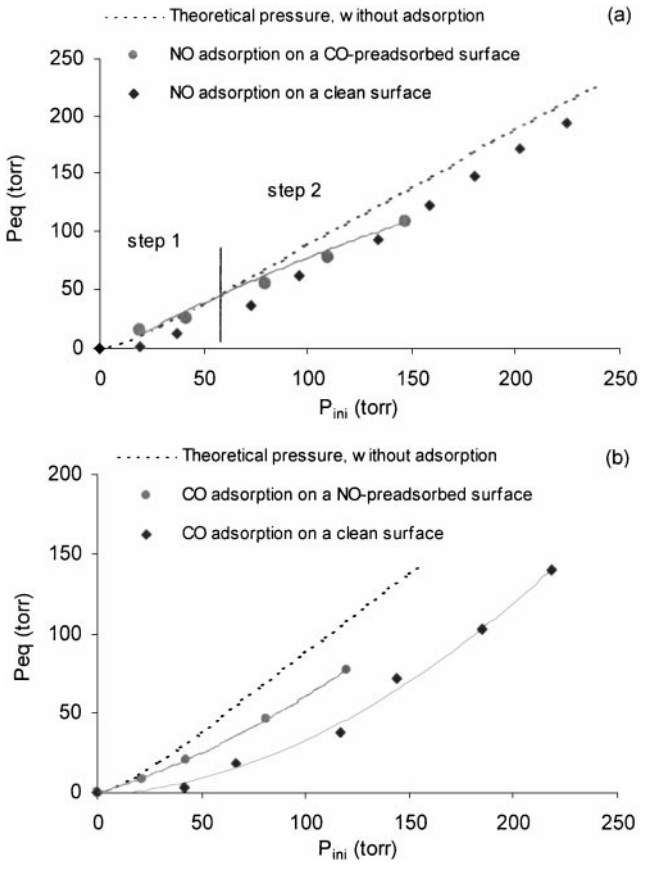

FIG. 6. Evolution (at 298 K for $Ni_{0.25}Cu_{0.80}Mn_{1.95}O_{4+\delta}$) of the equilibrium pressure P_{eq} with the initial pressure P_{ini} (before admission into the sample chamber) for (a) NO adsorption on a clean and a CO-preadsorbed surface and (b) CO adsorption on a clean and a NO-preadsorbed surface.

CO respectively as a function of the initial pressure P_{ini} (before admission of the gas into the sample chamber) in the cases of a clean and a CO (NO respectively) preadsorbed surface. The *theoretical* variation of pressure, i.e., without adsorption (only taking into account the gas expansion), is also reported in each figure with a dashed line for comparison.

As can be seen, both cases are distinct and will be dealt with separately.

In the case of a CO-preadsorbed surface (Fig. 6a), the experimental curve corresponding to NO adsorption may be divided into two successive steps: a first one (up to $P_{ini} \approx 60$ Torr) for which the experimental points fit the theoretical curve, meaning that the total number of gaseous molecules remains as if no adsorption occurred, and a second step where the curve slowly reaches the level obtained without CO preadsorption (which means that the NO uptake is no longer affected by the previous CO preadsorption). Moreover, in contrast to the adsorption on a clean surface where the pressure constantly decreases with time after admission of the adsorbate into the sample chamber, the pressure follows here a U-type variation with time as shown in Fig. 7. This behavior was observed for each experimental point of the first step of the $P_{eq} = f(P_{ini})$ curve of Fig. 6a. The variation of the pressure before reaching equilibrium shows that there is a first rapid uptake of NO (descending branch in Fig. 7) followed by a slower release of gaseous molecules up to equilibrium (ascending branch), corresponding to a return to the initial pressure. This implies that the number of gaseous molecules at equilibrium is the same as the initial one, and that the experimental points of the first step of Fig. 6a follow the theoretical curve as if there had not been any adsorption. Such a behavior could be explained by the rapid formation of a surface complex between CO preadsorbed molecules, as carbonyl or carbonate species (which are visible by IR) and NO adsorbate molecules. Such a complex has already been envisaged from IR studies by Panayotov *et al.* (12) in the case of NO and CO coadsorption on the spinel $CuCo_2O_4$. This complex, relatively unstable, could then decompose, leading to final NO adsorption and release of a carbon-containing molecule in the gas phase (CO or CO_2). However, step 2 in Fig. 6a shows that the equilibrium pressure finally reaches that obtained *without* CO preadsorption, showing apparently that the overall amount of the CO preadsorbed molecules has been replaced by NO. These results are also in accordance with the data of Table 2, which show a higher equilibrium coverage for NO than for CO. Thus, it can be inferred that (i) at least part of the NO and CO adsorption sites are common and (ii) NO is able to displace CO-preadsorbed molecules, which is in agreement with several other studies on NO/CO competitive adsorption (6, 13, 14).

CO adsorption on a NO-preadsorbed surface is completely different from the previous case. Indeed, Fig. 6b shows that the isotherm exhibits the classic shape of the adsorption on a clean surface, corresponding however to a CO uptake clearly inferior to that obtained without NO preadsorption. Moreover, in the present case, the adsorption kinetic curve $P = f(t)$ decreases, in a monotonous way, up to equilibrium like for adsorptions on clean surfaces, and does not display any U-type behavior, which allows us to exclude the formation of a complex surface intermediate between NO and CO molecules. These findings emphasize the difficulty, or even inability for CO to remove NO-preadsorbed molecules, as already observed by Yao and

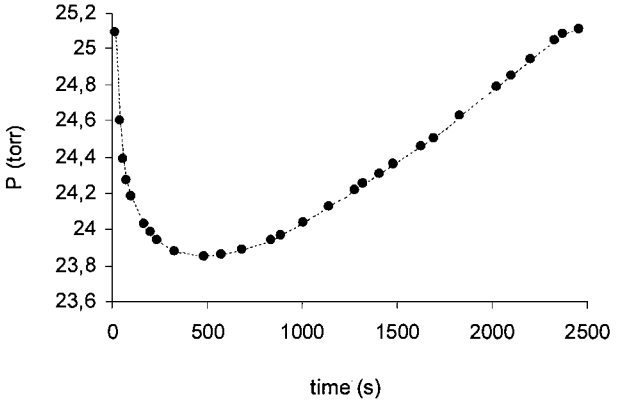

FIG. 7. Evolution of the pressure with time in the case of NO adsorption on a CO-preadsorbed surface of $Ni_{0.25}Cu_{0.80}Mn_{1.95}O_{4+\delta}$ at 298 K.

Shelef (6) on cobalt-containing spinels. However, as shown in Table 2, at the same temperature (298 K) the NO equilibrium coverage is higher than that of CO. The inability for CO to displace NO-preadsorbed molecules (up to saturation) should thus make it impossible for CO to adsorb, which is nevertheless the case. This apparent contradiction could be explained by the presence of some specific adsorption sites for CO. An *in situ* FT-IR study is presently in progress to determine the surface species formed upon adsorption of NO and/or CO on such surfaces and to better evaluate the interaction between the surface sites and these adsorbate molecules.

Kinetic Results

To determine the rate of the adsorption process of NO or CO molecules on the surface of such spinel oxides, the pressure drop taking place upon exposure of the samples to the adsorbate molecules was monitored as a function of time. The evolution of the number of NO or CO molecules adsorbed per gram of oxide (N_a) with time was then directly determined from the calibration of the volumes of the adsorption cell. The adsorption rates observed for NO and CO on a given oxide at constant initial pressure are of the same order of magnitude and give the same shape of kinetic curves. Figure 8a shows a typical example of

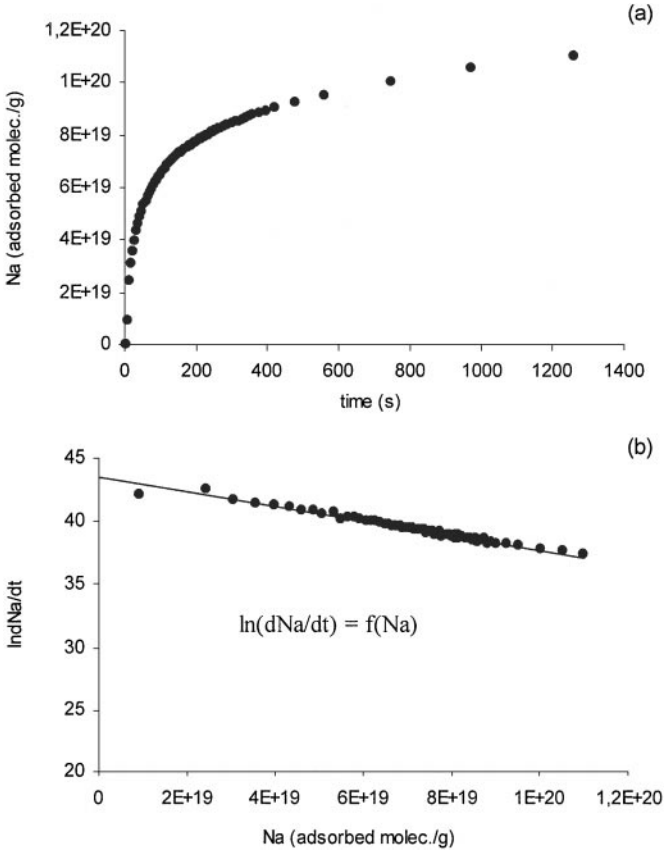

FIG. 8. Kinetic data for NO adsorption at 298 K on $Ni_{0.22}Cu_{0.57}Mn_{2.21}O_{4+\delta}$ as (a) $N_a = f(t)$ and (b) $\ln(dN_a/dt) = f(N_a)$.

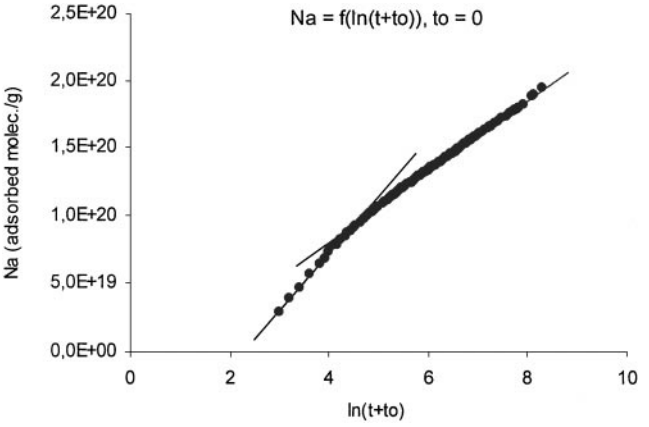

FIG. 9. Elovich plot $N_a = f(\ln(t + t_0))$ for NO adsorption on $Ni_{0.22}Cu_{0.57}Mn_{2.21}O_{4+\delta}$ at 298 K, taking $t_0 = 0$ (see text).

NO adsorption (weight sample = 250 mg and $P_{ini} = 190$ Torr) on $Ni_{0.22}Cu_{0.57}Mn_{2.21}O_{4+\delta}$ at room temperature.

The linearity of the plot $\ln(dN_a/dt)$ vs N_a (Fig. 8b) shows that the adsorption rate process follows the Elovich equation

$$\frac{dN_a}{dt} = a \cdot \exp(-b \cdot N_a(t)), \qquad [5]$$

where a and b are two constants. The integration of this equation gives a useful equation to analyze kinetic results:

$$N_a(t) = \frac{1}{b}\ln(ab) + \frac{1}{b}\ln(t + t_0). \qquad [6]$$

This integrated form introduces the time t_0 related to the pre-Elovichian period that often precedes the Elovichian rate process. Aharoni and Ungarish (15) have proposed a method for the determination of t_0 based on the extrapolation of t when Z tends to zero (where Z stands for the reciprocal of the adsorption rate). The application of this method to our kinetic data gave $t_0 \approx 0$, showing that this time can be neglected in a first approximation.

Figure 9 gives the plot of N_a vs $\ln(t + t_0)$ corresponding to the same example as above and taking $t_0 = 0$. Equation [6] shows that, for a rate process that follows an Elovich equation, this plot must be linear. However, two distinct linear branches are observed, revealing the existence of two distinct rate processes. If the same mathematical approach is run for CO adsorption, similar conclusions can be drawn, in particular, concerning the two Elovich linear branches for the plot of N_a vs $\ln(t + t_0)$. The occurrence of two adsorption rate processes has already been observed on similar adsorbate–adsorbent systems (16). In the present case, this could be interpreted assuming the existence of two kinds of adsorption sites with different surface accessibility or reactivity. Such hypotheses will have to be confirmed by additional experimental results.

CONCLUSION

The equilibrium adsorption of NO and CO molecules on non-stoichiometric nickel–copper spinel manganites was studied,

showing that these adsorptions follow the Freundlich model. The chemical composition of the oxides was found to have a great influence on the equilibrium coverage reached (N_a), and the logarithmic decrease of the adsorption heat of NO with N_a was determined from isotherms obtained at different temperatures. The adsorption of NO and CO on surfaces preadsorbed with CO and NO, respectively, were also investigated and the results showed the ability of NO to remove preadsorbed CO molecules whereas the contrary did not hold. Although an important part of the adsorption sites were found to be common for CO and NO, CO appeared to possess some specific sites. The transitory formation of a surface complex between CO-preadsorbed molecules and NO adsorbate molecules was assumed from kinetic results when the order of adsorptions was CO preadsorption–NO adsorption. Finally, the kinetics of adsorption of NO or CO molecules could precisely be described by the Elovich equation, with $t_0 \approx 0$, and two distinct rate processes were identified.

REFERENCES

1. Laberty, C., Alphonse, P., Demai, J. J., Sarda, C., and Rousset, A., *Mater. Res. Bull.* **32**(2), 249 (1997).
2. Laberty, C., Verelst, M., Lecante, P., Alphonse, P., Mosset, A., and Rousset, A., *J. Solid State Chem.* **129,** 271 (1997).
3. Drouet, C., Alphonse, P., and Rousset, A., *Solid State Ionics* **123,** 25 (1999).
4. Fritsch, S., Sarrias, J., Rousset, A., and Kulkarni, G. U., *Mater. Res. Bull.* **33**(8), 1185 (1998).
5. Oswald, H. R., and Wampetich, M. J., *Helv. Chim. Acta* **50,** 2023 (1967).
6. Yao, H. C., and Shelef, M., *J. Phys. Chem.* **78,** 2490 (1974).
7. Shelef, M., *Catal. Rev.-Sci. Eng.* **11**(1), 1 (1975).
8. Tascón, J. M. D., and Tejuca, L. G., *Z. Phys. Chem. Neue Folge* **121,** 79 (1980).
9. Dushman, S., "Scientific Foundations of Vacuum Technique." Wiley, New York, Chapman & Hall, London, 1949.
10. Halsey, G., *Adv. Catal.* **4,** 295 (1952).
11. Peña, M. A., Tascón, J. M. D., Fierro, J. L. G., and Tejuca, L. G., *J. Colloid Interface Sci.* **119**(1), 100 (1987).
12. Panayotov, D., Matyshak, V., Sklyarov, A., Vlasenko, A., and Mehandjiev, D., *Appl. Catal.* **24,** 37 (1986).
13. Tascón, J. M. D., Tejuca, L. G., and Rochester C., *J. Catal.* **95,** 558 (1985).
14. Raskó, J., and Solymosi, F., *Acta. Chim. Acad. Sci. Hung.* **95**(4), 389 (1977).
15. Aharoni, C., and Ungarish, M., *J. Chem. Soc. Faraday Trans. 1* **72,** 400 (1976).
16. Otto, K., and Shelef, M., *J. Catal.* **14,** 226 (1969).